Research Article

Analysis of vibration signals caused by ball bearing defects using time-domain statistical indicators

Prashant H. Jain[1, 2*] and Santosh P. Bhosle[3]
Research Scholar, Maharashtra Institute of Technology, Aurangabad, India[1]
Assistant Professor, T.P.C.T's College of Engineering, Osmanabad, India[2]
Professor and Director, Maharashtra Institute of Technology, Aurangabad, India[3]

Abstract
Ball bearings are widely used for providing support to the rotating parts in machinery and vehicles. Any damage to a bearing element during operation leads to vibration and catastrophic failure. Therefore, it is essential to monitor the condition of bearing elements during operations to detect early the occurrence and propagation of defects in bearing elements. Thus, we are motivated to identify the best condition indicator for detecting bearing defects and tracking their progression. The objective of this paper is to study and analyze the effects of different types of bearing defects and their sizes on bearing vibration responses, using different time-domain statistical indicators, and to determine the best indicator for detecting bearing defects and the evolution of defect sizes. In this paper, vibration signals obtained from normal and defective bearings are analyzed by using six traditional time-domain statistical indicators (TDSIs); peak, root mean square, crest factor, kurtosis, impulse factor and shape factor. Also, six new indicators developed by other researchers, namely TALAF, THIKAT, "kurtosis, crest factor and root mean square (KUCR)", engineering condition indicator (ECI), SIANA, and INTHAR, are used to analyze the vibration signals. In addition, the effects of shaft speed on vibration responses are analyzed for a normal bearing using all these indicators. Vibration signals of bearings are obtained from the bearing datasets which are made available by the bearing data center of Case Western Reserve University (CWRU). A MATLAB code is developed to obtain TDSIs and new indicators from the data sets. In the results, it is found that KUCR is the most sensitive indicator to the detection of incipient defects and evolution of defect size; however, shape factor and TALAF are less sensitive to defect size detection.

Keywords
Vibration signal analysis, Time-domain statistical indicators, Condition indicators, Bearing defects, CWRU bearing data.

1.Introduction

Deep groove ball bearings are commonly used in industries and in automobiles to support the rotating shafts. Balls, outer race and inner race are the important elements of deep groove ball bearing. Any defect on these elements, i.e., ball defect (BD), outer race defect (ORD) or inner race defect (IRD) causes unwanted noise and vibration. To determine the exact location of bearing defect and its intensity, several techniques of vibration signal analysis (VSA) are available, which are basically divided into time domain, frequency domain, and time frequency domain [1].

In time domain analysis technique, different traditional TDSIs are used for vibration analysis, which involves peak, peak-to-peak, mean, root mean square, crest factor, skewness, kurtosis, clearance factor, impulse factor, shape factor, etc. [1].

Among all the time-domain statistical indicators (TDSIs), the peak, root mean square, crest factor, kurtosis, impulse factor and shape factor are widely used for ball bearing defect analysis [2]. In this study, the effectiveness of these widely used TDSIs is compared to the evolution of bearing defect sizes.

Peak is the maximum amplitude of the signal. Root mean square (RMS) is the square root of mean square of the signal. It measures the overall vibration level of the signal. Crest factor (CF) is the ratio of peak and RMS of the signal, which shows the spikiness of

---

*Author for correspondence

the vibration signal. Kurtosis (KUR) is the measure of peakedness of the probability density function of a time series. Impulse factor (IF) is the ratio of peak and the absolute mean of the signal. Shape factor (SF) is the ratio of RMS and the absolute mean of the signal. *Table 1* shows the equations of these traditional time-domain statistical indicators as given by [3, 4].

Table 1 Equations of some of the traditional time-domain statistical indicators

Indicators	Equations
Peak	$\lvert x_{\max} \rvert$
Root Mean Square (RMS)	$\sqrt{\dfrac{1}{N}\sum_{i=1}^{N}(x_i)^2}$
Crest factor (CF)	$\dfrac{\text{Peak}}{\text{RMS}}$
Kurtosis (KUR)	$\dfrac{\dfrac{1}{N}\sum_{i=1}^{N}(x_i - x)^4}{\left(\dfrac{1}{N}\sum_{i=1}^{N}(x_i - x)^2\right)^2}$
Impulse factor (IF)	$\dfrac{\text{Peak}}{\dfrac{1}{N}\sum_{i=1}^{N}\lvert x_i \rvert}$
Shape factor (SF)	$\dfrac{\text{RMS}}{\dfrac{1}{N}\sum_{i=1}^{N}\lvert x_i \rvert}$

here x_i = Signal's instantaneous amplitude, N = No. of samples and $\bar{x}$ is the mean of the signal

Although, these TDSIs are capable of distinguishing the healthy and defective bearings [3], there is always a need to find the best and effective indicator for diagnosis of defects in bearings and which is more sensitive to the defect size. For the sake of improving the bearing defect detection ability, some researchers [2], [4−11] developed new indicators using a combination of traditional TDSIs for bearing defect detection. These new indicators developed by researchers include 'TALAF' and 'THIKAT' [2], 'KUCR' [5], 'engineering condition indicator (ECI)' [6], 'SIANA' and 'INTHAR' [7], 'combined function of crest factor, root mean square, impact factor and standard deviation (CRIS)' [8], 'NM^2_a' and 'NM^3_a' [9], ''S$_\alpha$'' [10], 'KR (Kurtosis × RMS)', 'KP (Kurtosis × Peak)' and 'RP (RMS × Peak)' [11]. In the current study, some of the new indicators developed by researchers [2], [5−7] are used for comparison. *Table 2* shows the equations of these newly developed indicators. A complete list of abbreviations is shown in *Appendix I*.

Table 2 Equations of some newly developed indicators by the researchers

Indicators	Equations
TALAF	$\log\left[\text{KUR} + \dfrac{\text{RMS}}{\text{RMS}_0} \right]$
THIKAT	$\log\left[\text{KUR}^{\text{CF}} + \left(\dfrac{\text{RMS}}{\text{RMS}_0} \right)^{\text{Peak}} \right]$
KUCR	$\sqrt{\text{KUR}^2 + \left(\text{CF} \times \dfrac{\text{RMS}}{\text{RMS}_0} \right)^2}$
ECI	$\dfrac{N\sum_{i=1}^{N}(x_i - x)^4}{\sum_{i=1}^{N}(x_i - x)^2}$
SIANA	$\log\left[\dfrac{\text{CF}^{\text{KUR}}}{\text{Peak}^{\text{RMS}}} \right]$
INTHAR	$\log\left[\dfrac{\text{Peak}^{\text{KUR}}}{\text{CF}^{\text{RMS}}} \times \text{IF} \right]$

here RMS_0 = RMS of normal bearing

Among all the indicators shown in *Table 1* and *Table 2*, the peak and RMS are the dimensional indicators which have the same unit as the amplitude, while other indicators are non-dimensional indicators [7, 12].

In the current work, the effects of different types of bearing defects and their sizes on vibration responses are analyzed using six traditional TDSIs and six newly developed indicators by researchers. Also, the sensitivity of these indicators in bearing defect detection and evolution of defect size is analyzed.

This paper is organized as follows: the literature review on use of TDSIs and new indicators in the diagnosis of bearing defects presented by researchers is discussed in section 2. The method used for obtaining the vibration responses in terms of various indicators from the normal and defective bearings is presented in section 3. In section 4, the results obtained from the normal and defective bearing data by using MATLAB code is discussed and presented in tabular form. The effects of speed and defect size on vibration responses are discussed in section 5 along with the limitations. Conclusions and the future work are discussed in section 6.

2.Literature review

Recently, Jain and Bhosle [13] reviewed the literature on traditional and new TDSIs used for diagnosis of

rolling element bearing defects. In their conclusions, they stated the performance of TDSIs in bearing defect detection at different operating conditions. They found that all indicators detect the defects and their growth with more or less sensitivity.

In the last few decades, many researchers used TDSIs for bearing defect detection. Some of them analyzed the effectiveness of traditional TDSIs for diagnosis of bearing defects and to identify the defect severity as discussed below.

Dyer and Stewart [14] demonstrated the first use of kurtosis in bearing fault diagnosis. They showed that the kurtosis of a good bearing is close to 3 and increases as the size of the defect increases. They also showed that when the defect size increases further, then kurtosis comes down to 3.

Tandon [15] compared the effectiveness of only three TDSIs, i.e., peak, RMS and CF for detection of bearing defects and their sizes. They observed that the values of peak and RMS due to ORD are greater than due to IRD, but, CF due to IRD is greater than due to ORD.

Patil et al. [16] used only two TDSIs, i.e., CF and kurtosis, and studied the effects of an increase in speed and ORD size of bearing vibration using these two indicators. They have not considered other types of defects. They found that CF and kurtosis are effective in defect detection at lower speeds.

Utpat et al. [17] also studied the effectiveness of only three TDSIs, i.e., peak-to-peak, peak and RMS in bearing fault diagnosis. They studied their effects at different speeds and loads. They found that the defect (ORD, IRD and BD) detection ability of peak-to-peak value is best followed by peak and RMS.

Chebil et al. [18] compared nine TDSIs, i.e., mean, standard deviation, clearance factor and six indicators as mentioned in *Table 1* for defect size detection. They found that peak, RMS and CF are good indicators of incipient bearing defects of any type (ORD, IRD and BD).

Wang et al. [19] compared seven TDSIs, i.e., peak-to-peak, RMS, shape factor, impulse factor, kurtosis, CF and clearance factor for defection and evolution of ORD. They found that peak-to-peak, RMS and kurtosis distinguish well the moderate and severe ORDs of bearing. They have not considered diagnosis of IRDs and BDs.

Sharma et al. [20] compared ten features including five TDSIs, i.e., standard deviation, RMS, CF, skewness and kurtosis for evolution of defect size of a ball bearing. They found that all TDSIs are sensitive to the increase in defect sizes of any type (ORD, IRD and BD).

Shukla et al. [3] compared the effectiveness of sixteen traditional TDSIs for distinguishing the normal and defective ball bearings. They found that for all types of bearing defects the peak-to-peak, kurtosis factor, square root of amplitude, RMS and standard deviation are the best indicators, and kurtosis, clearance factor and margin factor are the worst indicators.

Wu [12] compared six TDSIs, i.e., variance, RMS, kurtosis, margin factor, impulse factor and CF, for tracking the evolution of various bearing defects. They found that TDSIs are capable to identify subtle changes in the bearings due to incipient defects and are able to track the evolution of bearing defect efficiently.

Singh and Harsha [21] compared the effectiveness of RMS, skewness, kurtosis and CF in bearing fault diagnosis. They investigated that the CF and kurtosis of ORD are highly sensitive, whereas skewness of ORD is not sensitive to the load and speed variations. They also found that RMS and skewness are not able to diagnose the bearing defects.

Yadav and Pahuja [22] compared six TDSIs, namely, mean, peak, RMS, CF, skewness and kurtosis for diagnosis of bearing defects. They stated that peak, RMS, skewness and kurtosis identify any type of bearing defects more reliably.

Many other researchers [5, 8], [23−35] also used traditional TDSIs for diagnosis of bearing defects.

Some of the researchers developed new indicators by using the combinations of traditional TDSIs as discussed below.

Sassi et al. [2] presented two new indicators called 'TALAF' and 'THIKAT', and compared these new indicators with traditional TDSIs mentioned in *Table 1*. They showed the effectiveness of TALAF indicator for ORD size defection. They found that TALAF increases constantly with an increase in ORD size. In their study, they have not studied the effects of IRD and BD on the bearing.

Pradhan and Gupta [5] developed a new indicator called 'KUCR' and compared KUCR with traditional TDSIs mentioned in *Table 1*. They showed the effectiveness of KUCR for detection of IRD and BD. They found that KUCR increases constantly with increase in size of IRD and BD. They have not considered ORD of bearing in their analysis.

Hu et al. [6] developed a new indicator 'ECI', which is a product of kurtosis and variance of the signal. ECI is the representation of kurtosis and energy of the vibration signal. They compared the performance of ECI with RMS, crest factor and kurtosis in diagnosis of ORDs present in wind turbine bearings and showed the effectiveness of ECI.

Salem et al. [7] presented two new indicators 'SIANA' and 'INTHAR' and showed that these indicators are highly sensitive to the defect growth. They also compared the traditional TDSIs mentioned in *Table 1* for defect size detection. They found that peak is more sensitive than RMS and when the indicators are normalized, the kurtosis and peak are more sensitive than other TDSIs. They have not studied the effects of BD on the bearing.

Paliwal et al. [8] proposed a new indicator 'CRIS', which is a created by combining CF, RMS, IF and standard deviation. They showed that CRIS can be used effectively for bearing defect severity detection of any type of defect on bearing, i.e., ORD, IRD and BD.

Niu et al. [9] presented new normalized statistical moments, i.e., NM^2_a and NM^3_a. These two indicators are the modified functions of the vibration signal amplitude and number of samples. They compared these two indicators with skewness and kurtosis for all types of bearing defect detection and found that new indicators are as effective as skewness and kurtosis.

Tao et al. [10] presented an indicator named as 'S_α', which is same as the indicator NM^2_a, which is presented by Niu et al. [9]. They compared the new indicator with kurtosis and Honarvar third moment Sr for bearing defect detection.

Jain and Bhosle [11] used products of kurtosis, peak and RMS as new indicators to distinguish the defective bearing from normal bearing and to study the effects of the increase in radial load. They compared the results of these indicators with peak, RMS, CF, skewness, kurtosis, TALAF and THIKAT.

They demonstrated that these indicators clearly distinguish the defective bearing from the normal bearing, as well as distinguished bearings with ORD from the bearings with IRD. But, they have not analyzed the effects of defect size growth in their study.

Bastami and Vahid [36] introduced statistical parameter called 'Level crossing rate' (LCR), which measures how often a vibration signal crosses a specific threshold value. They compared the results of the LCR with peak, RMS, CF and kurtosis in the detection of ORD, IRD and BD in bearings. They demonstrated that LCR shows bilinear relation with defect size and hence useful for diagnosis and prognosis of bearings.

Literature review shows that many researchers have studied the effectiveness of traditional TDSIs for bearing defect detection. Also, it is seen that few researchers compared their newly developed indicators with the traditional TDSIs for the detection of bearing defects and evolution defect size. But, no literature is found on comparison of all traditional and newly developed indicators for finding the effectiveness in the detection of bearing defects and the evolution of defect size. This paper presents the VSA of ball bearings having different types of defects and different sizes of defects by using commonly used traditional TDSIs and newly developed condition indicators. In the results, it is found that most of the indicators distinguish the defective bearing from the normal bearing, hence useful for bearing condition monitoring, and KUCR is the most sensitive indicator for detection of bearing defects and the evolution of defect size.

3.Methods
In this study, datasets of ball bearing vibration signal, which are provided by Case Western Reserve University (CWRU) on their website [37] are used for VSA of ball bearing. These dataset files are available in MATLAB format with .mat extension. From these datasets, 48 datasets are used in this work. Out of these 48 datasets, 4 datasets are of normal bearings and 44 datasets are of defective bearings having defects on different bearing elements, i.e., on outer race, inner race and ball. *Table 3* shows the specification of SKF 6205-2RS JEM ball bearing and equivalent new technology network (NTN) bearing used for obtaining vibration datasets.

Table 3 Specifications of SKF and NTN made deep groove ball bearing used for vibration datasets

Inner diameter d (mm)	Outer diameter D (mm)	Width W (mm)	Ball diameter D_b (mm)	Cage diameter D_c (mm)	No. of Balls n
25	52	15	7.94	39.04	9

Tables 4 and *5* shows 4 datasets of normal bearings and 44 datasets of defective bearings used in this analysis, respectively. In these tables, for simplicity, new codes are given for the bearing datasets downloaded from the CWRU data center. Each code consists of 4 groups of alphanumeric characters. First group indicate the file name of downloaded .mat file. Second group (i.e., 12DE) indicate drive end bearing with 12000 Hz sampling frequency. Third group indicate the bearing status, i.e., normal or defective with defect diameter. For example, BD14 indicate a ball defect with defect diameter 0.014 inches. Fourth group indicate the speed of the motor in rpm. Three types of defects, i.e., IRD, BD and ORD, were created on 9 SKF 6205-2RS JEM bearings and on 2 equivalent NTN bearings. In 9 SKF bearings, 3 bearings have IRDs, 3 bearings have BDs, and 3 bearings have ORDs. Each defect type consists of 3 different diameters having the same depth of 0.011-inch (0.279 mm). 3 defect diameters consist of 0.007-inch (0.178 mm), 0.014-inch (0.356 mm), and 0.021-inch (0.533 mm). In 2 NTN bearings, one bearing has an IRD, and the other has a BD. The IRD is of

diameter 0.028-inch (0.711 mm) with a depth of 0.05-inch (1.27 mm), and BD is of the same diameter with a depth of 0.15-inch (3.81 mm). All defects were created on 11 bearings using electro-discharge machining (EDM).

Table 4 Datasets of normal bearings provided by CWRU with new codes

Speed	Normal bearing dataset codes
1797	97 12DE Normal 1797
1772	98 12DE Normal 1772
1750	99 12DE Normal 1750
1730	100 12DE Normal 1730

Figure 1 shows sample computer aided drawings of circular defects of 0.533 mm diameter and 0.2794 mm depth made on the outer race, inner race and a ball of SKF 6205-2RS JEM ball bearing. During rotation of the shaft, whenever a defect on a bearing surface comes into contact with the adjacent bearing surface, an impulse of vibration is generated. *Figure 2* shows the impulse generation mechanism due to ORD, IRD and BD on the ball bearing.

Table 5 Datasets of defective bearings provided by CWRU with new codes

Defect diameter and bearings	Speed (RPM)	Inner RACE defect dataset codes	Ball defect dataset codes	Outer RACE Defect (In load zone) dataset codes
0.007 inch (0.178 mm) 3 SKF Bearings	1797	105 12DE IRD7 1797	118 12DE BD7 1797	130 12DE 6ORD7 1797
	1772	106 12DE IRD7 1772	119 12DE BD7 1772	131 12DE 6ORD7 1772
	1750	107 12DE IRD7 1750	120 12DE BD7 1750	132 12DE 6ORD7 1750
	1730	108 12DE IRD7 1730	121 12DE BD7 1730	133 12DE 6ORD7 1730
0.014 inch (0.356 mm) 3 SKF Bearings	1797	169 12DE IRD14 1797	185 12DE BD14 1797	197 12DE 6ORD14 1797
	1772	170 12DE IRD14 1772	186 12DE BD14 1772	198 12DE 6ORD14 1772
	1750	171 12DE IRD14 1750	187 12DE BD14 1750	199 12DE 6ORD14 1750
	1730	172 12DE IRD14 1730	188 12DE BD14 1730	200 12DE 6ORD14 1730
0.021 inch (0.533 mm) 3 SKF Bearings	1797	209 12DE IRD21 1797	222 12DE BD21 1797	234 12DE 6ORD21 1797
	1772	210 12DE IRD21 1772	223 12DE BD21 1772	235 12DE 6ORD21 1772
	1750	211 12DE IRD21 1750	224 12DE BD21 1750	236 12DE 6ORD21 1750
	1730	212 12DE IRD21 1730	225 12DE BD21 1730	237 12DE 6ORD21 1730
0.028 inch (0.711 mm) 2 NTN Bearings	1797	3001 12DE IRD28 1797	3005 12DE BD28 1797	Not Available
	1772	3002 12DE IRD28 1772	3006 12DE BD28 1772	Not Available
	1750	3003 12DE IRD28 1750	3007 12DE BD28 1750	Not Available
	1730	3004 12DE IRD28 1730	3008 12DE BD28 1730	Not Available

Figure 3 shows the test setup for bearing defect vibration data collection provided by CWRU. Datasets used in this paper are taken from the test bearing of SKF made having number 6205-2RS JEM, which is located at the drive end (DE) of the motor shaft. All the datasets were recorded by using a 16-

channel digital audio tape (DAT) recorder at 12000 sampling frequency for the speed range between 1730 to 1797 rpm and for a duration of 10 seconds. Datasets of ORD located at the center of the load zone, i.e., at 6 o'clock position, are considered for this study. Among all bearing vibration datasets

publicly available on the internet, many researchers used the bearing vibration datasets provided by CWRU in their research work as standard reference datasets [38]. Due to this reason, in this work, the authors used CWRU bearing datasets for analysis of bearing vibration.
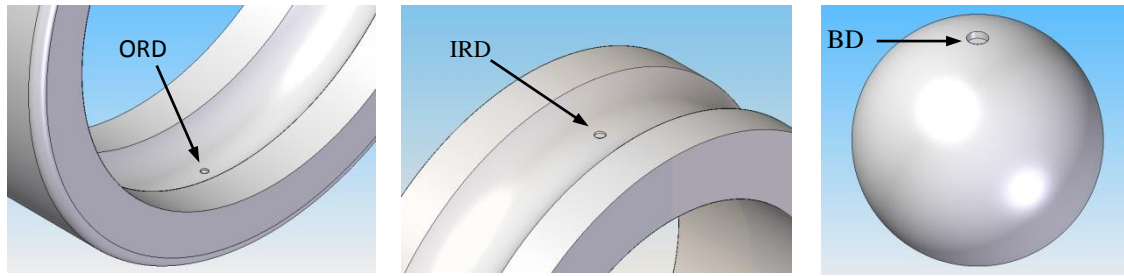

Figure 1 Computer aided drawings of defects made on a) outer race, b) inner race and c) a ball of SKF bearing
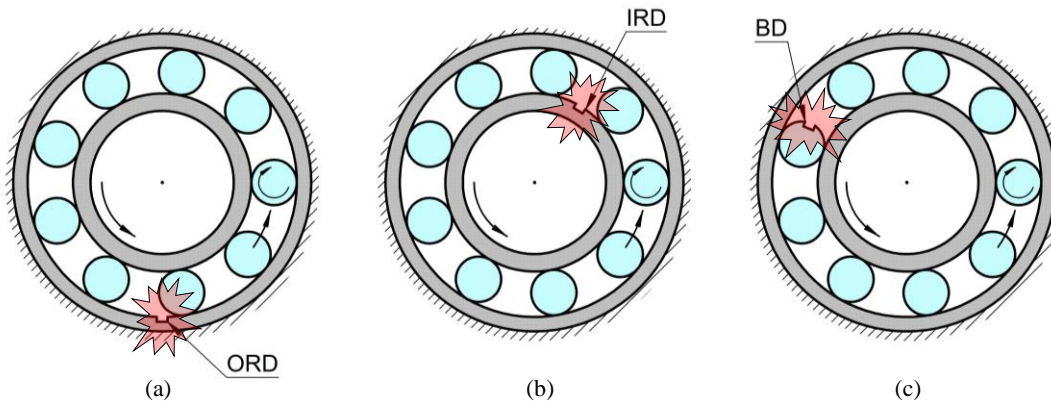

Figure 2 Impulse generation in bearings due to a) outer race defect, b) inner race defect and c) ball defect
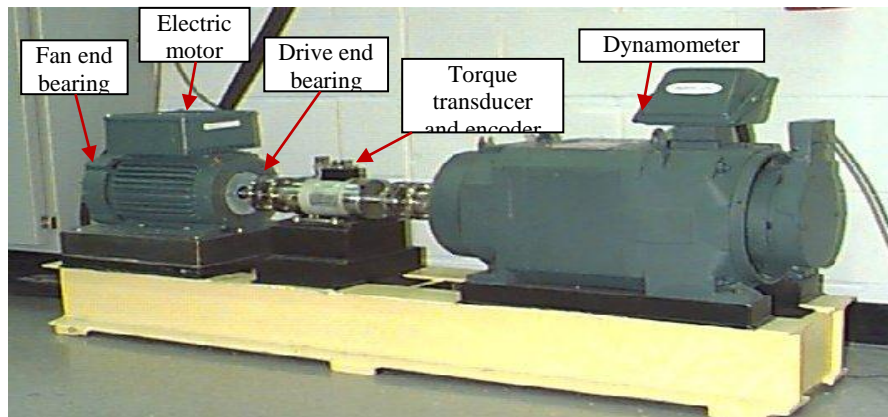

Figure 3 Test setup of CWRU for bearing vibration data collection

First MATLAB code is developed to separate the acceleration signals from .mat files of each dataset and to store them in .csv files with new dataset codes as shown in *Tables 4* and *5*. Second MATLAB code is developed to plot time waveforms and envelope spectrums for each dataset in *Tables 4* and *5*. Third MATLAB code is developed to determine the values of different statistical parameters shown in *Tables 1* and 2 from each dataset presented in *Tables 4* and *5*.

705

4.Results

To analyze the effects of speed and defect sizes on bearing vibration responses using TDSIs, the datasets provided by CWRU are processed using MATLAB codes (as discussed in Section 3) and obtained values of statistical indicators are presented in *Tables 6* and *7*. These tables show the values of all traditional and new indicators calculated for the datasets of normal

bearings and defective bearings, respectively, shown in *Tables 4* and *5*. These values are calculated by using MATLAB codes from 48 datasets by using equations shown in *Tables 1* and *2* for different motor speeds, i.e., 1730, 1750, 1772 and 1797 rpm. The values obtained for traditional indicators in this work also match the values obtained by the researchers [5, 39]. This validates the results obtained in this work.

To analyze the effects of change in speed on vibration responses using statistical indicators for normal bearing, 4 datasets provided by CWRU for normal bearings at different speeds are used. These datasets for speeds different speeds, i.e., for 1730 rpm, 1750 rpm, 1772 rpm and 1797 rpm, are given in *Table 4*.

Table 6 Values of all indicators for normal bearing for different speeds

Bearing	SPEED	PEAK	RMS	CF	KUR	IF	SF	TALAF	THIKAT	KUCR	ECI	SIANA	INTHAR
	1730	0.284	0.066	4.306	2.957	5.360	1.245	0.597	2.032	5.224	0.013	1.911	-0.931
Normal Bearing	1750	0.359	0.064	5.585	2.925	6.925	1.240	0.594	2.604	6.304	0.012	2.214	-0.508
with no defects	1772	0.318	0.066	4.785	2.931	5.938	1.241	0.594	2.237	5.611	0.013	2.026	-0.732
	1797	0.311	0.074	4.220	2.764	5.232	1.240	0.576	1.869	5.044	0.015	1.766	-0.728

Table 7 Values of all indicators for defective bearings for different defect sizes and different speeds

Defect Diameter	SPEED	PEAK			RMS			CF			KUR		
		IRD	BD	ORD	IRD	BD	ORD	IRD	BD	ORD	IRD	BD	ORD
0.007"	1730	1.672	0.672	3.236	0.314	0.154	0.580	5.330	4.371	5.576	5.291	2.890	7.964
(0.178 mm)	1750	1.640	0.605	3.101	0.300	0.147	0.570	5.474	4.106	5.439	5.564	2.831	7.852
	1772	1.581	0.640	3.112	0.293	0.139	0.592	5.397	4.600	5.258	5.542	2.964	7.595
	1797	1.739	0.604	3.630	0.292	0.139	0.670	5.965	4.338	5.423	5.396	2.985	7.649
0.014"	1730	2.127	1.989	0.665	0.181	0.134	0.095	11.765	14.879	7.022	18.164	14.859	3.797
(0.356 mm)	1750	1.854	1.839	0.477	0.163	0.144	0.097	11.371	12.820	4.931	21.686	9.752	3.024
	1772	2.030	1.340	0.396	0.166	0.141	0.094	12.265	9.510	4.230	22.084	8.837	2.940
	1797	1.934	2.278	0.551	0.198	0.153	0.101	9.778	14.918	5.469	21.957	17.769	3.056
0.021"	1730	3.615	0.576	6.653	0.449	0.118	0.559	8.056	4.886	11.901	8.345	3.106	23.542
(0.533 mm)	1750	3.623	0.646	6.653	0.489	0.107	0.570	7.411	6.018	11.672	8.058	3.301	23.164
	1772	3.686	1.475	6.207	0.442	0.129	0.561	8.343	11.427	11.057	7.667	9.407	21.971
	1797	3.788	1.660	6.653	0.525	0.136	0.583	7.210	12.238	11.408	7.445	8.549	21.006
0.028"	1730	4.347	11.364	NA	0.823	2.145	NA	5.281	5.298	NA	3.317	3.899	NA
(0.711 mm)	1750	4.541	10.442	NA	0.841	2.146	NA	5.397	4.867	NA	3.286	3.772	NA
	1772	3.931	11.674	NA	0.838	2.030	NA	4.693	5.751	NA	3.196	3.910	NA
	1797	4.785	10.931	NA	0.838	2.077	NA	5.707	5.263	NA	3.397	3.872	NA

Defect Diameter	SPEED	IF			SF			TALAF			THIKAT		
		IRD	BD	ORD	IRD	BD	ORD	IRD	BD	ORD	IRD	BD	ORD
0.007"	1730	7.458	5.450	9.109	1.399	1.247	1.634	1.002	0.718	1.225	3.857	2.022	5.029
(0.178 mm)	1750	7.673	5.108	8.862	1.402	1.244	1.629	1.010	0.709	1.223	4.081	1.866	4.873
	1772	7.613	5.752	8.493	1.411	1.250	1.615	0.998	0.704	1.218	4.014	2.175	4.639
	1797	8.326	5.433	8.948	1.396	1.253	1.650	0.971	0.688	1.223	4.367	2.065	4.812
0.014"	1730	18.415	21.638	8.921	1.565	1.454	1.270	1.320	1.228	0.719	14.814	17.438	4.069
(0.356 mm)	1750	18.785	18.224	6.188	1.652	1.422	1.255	1.384	1.079	0.656	15.193	12.680	2.372
	1772	20.484	13.636	5.285	1.670	1.434	1.249	1.391	1.040	0.638	16.486	9.000	1.986
	1797	16.569	22.680	6.859	1.695	1.520	1.254	1.392	1.298	0.645	13.117	18.643	2.654
0.021"	1730	11.900	6.160	24.400	1.481	1.260	2.054	1.181	0.690	1.505	7.423	2.407	16.326
(0.533 mm)	1750	11.100	7.630	23.800	1.500	1.268	2.036	1.195	0.696	1.506	6.716	3.121	15.930
	1772	12.332	15.600	22.200	1.478	1.361	2.007	1.156	1.055	1.483	7.380	11.124	14.837
	1797	10.525	16.400	22.600	1.460	1.343	1.979	1.163	1.016	1.461	6.287	11.404	15.085
0.028"	1730	6.720	7.012	NA	1.273	1.324	NA	1.199	1.562	NA	4.771	17.189	NA
(0.711 mm)	1750	6.840	6.406	NA	1.267	1.316	NA	1.214	1.570	NA	5.073	15.907	NA
	1772	5.930	7.610	NA	1.264	1.324	NA	1.199	1.538	NA	4.332	17.339	NA
	1797	7.280	6.970	NA	1.276	1.325	NA	1.169	1.505	NA	5.054	15.843	NA

Defect Diameter	SPEED	KUCR			ECI			SIANA			INTHAR		
		IRD	BD	ORD	IRD	BD	ORD	IRD	BD	ORD	IRD	BD	ORD
0.007"	1730	25.910	10.589	49.748	0.520	0.068	2.683	3.775	1.878	5.647	1.825	0.138	4.588
(0.178 mm)	1750	26.098	9.823	48.870	0.499	0.061	2.553	4.044	1.769	5.495	1.859	-0.001	4.388
	1772	24.444	10.081	47.479	0.475	0.057	2.661	4.000	1.991	5.183	1.769	0.093	4.247
	1797	24.172	8.709	49.783	0.459	0.058	3.429	4.115	1.932	5.241	1.991	-0.007	4.743

		PEAK	RMS	CF	KUR	IF	SF	TALAF	THIKAT	KUCR	ECI	SIANA	INTHAR
0.014" (0.356 mm)	1730	37.037	33.645	10.782	0.594	0.266	0.034	19.387	17.383	3.231	7.025	5.616	0.198
	1750	36.086	30.227	8.016	0.577	0.201	0.028	22.852	10.766	2.127	6.917	3.682	-0.247
	1772	37.713	22.031	6.648	0.605	0.175	0.026	23.992	8.627	1.879	7.923	2.120	-0.519
	1797	34.189	35.616	8.063	0.859	0.414	0.031	21.686	20.801	2.281	7.315	7.531	-0.030
0.021" (0.533 mm)	1730	55.483	9.283	103.660	1.680	0.043	7.356	7.311	2.168	24.861	5.328	-0.035	20.162
	1750	56.924	10.571	106.029	1.926	0.038	7.526	6.736	2.593	24.250	5.126	0.171	19.832
	1772	56.036	24.128	96.031	1.496	0.157	6.925	6.813	9.931	22.484	5.028	2.642	18.181
	1797	51.868	24.056	92.567	2.055	0.157	7.145	6.083	9.268	21.728	4.878	2.949	18.026
0.028" (0.711 mm)	1730	66.045	172.490	NA	2.247	17.940	NA	1.872	0.559	NA	2.349	3.408	NA
	1750	70.695	162.440	NA	2.326	17.368	NA	1.853	0.406	NA	2.379	3.175	NA
	1772	59.286	175.862	NA	2.242	16.112	NA	1.648	0.805	NA	2.111	3.513	NA
	1797	64.927	148.166	NA	2.388	16.703	NA	1.999	0.635	NA	2.537	3.366	NA

Table 8 shows the average values of all the indicators for the normal bearings at different motor speeds as given in *Table 6*.

Figure 4 shows changes in the values of all indicators at different speeds for normal bearing.

Table 8 Average values of all indicators at different speeds for normal bearing

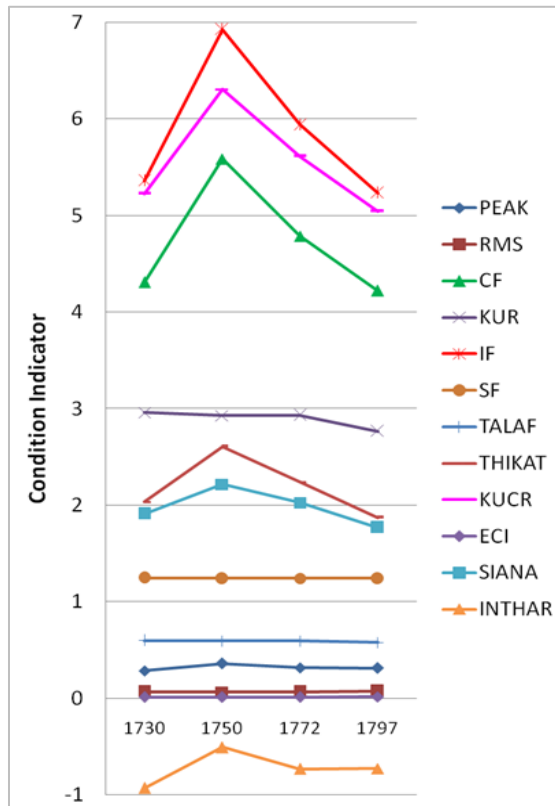| Indicators	PEAK	RMS	CF	KUR	IF	SF	TALAF	THIKAT	KUCR	ECI	SIANA	INTHAR
Averages	0.318	0.068	4.724	2.894	5.864	1.242	0.590	2.186	5.546	0.013	1.979	−0.725

Figure 4 Values of indicators for normal bearing at different speeds

To analyze the effects of defect sizes on vibration responses using statistical indicators, 44 datasets provided by CWRU for defective bearings at different speeds are used. These datasets for different speeds, i.e., for 1730 rpm, 1750 rpm, 1772 rpm and 1797 rpm, are given in *Table 5*.

Figure 4 show that the minimum speed is 1730 rpm and the maximum speed is 1797 rpm, i.e., the speed range is only 67 rpm, which is very small. Therefore, there is not much variation in the values of statistical indicators obtained in this range of speed.

From *Table 8,* it is observed that the average values of all indicators at different speeds for normal bearing are near to the values of indicators obtained for a speed of 1772 rpm (*Table 6*). Therefore, the indicator values for defective bearings at speed 1772 rpm are considered for analysis of effects of defect sizes on statistical indicators.

Figure 5 shows the sample time waveforms of normal and defective bearings running at a constant motor speed of 1772 rpm. The defective bearings have defects of different diameters on the inner race, ball and outer race of the bearings. The datasets are obtained for durations of 10 seconds. In *Figure 5*, the peaks of time waveforms for each defective bearing are also shown. The amplitudes of these peaks are the same as the peak values calculated by using MATLAB code '|xmax|' for the datasets of normal and defective bearings given in *Tables 4* and *5*. These calculated peak values are presented in *Tables 6* and *7*. From *Figure 5,* it is clear that for all types of defects in bearing and for all sizes of defects, the vibration levels are more than that of the normal bearing. *Table 9* shows the values of all statistical indicators obtained for the normal and defective bearings for a constant speed of 1772 rpm. *Figure 6* shows the graphs of traditional statistical indicators for different IRD sizes and for different motor speeds.
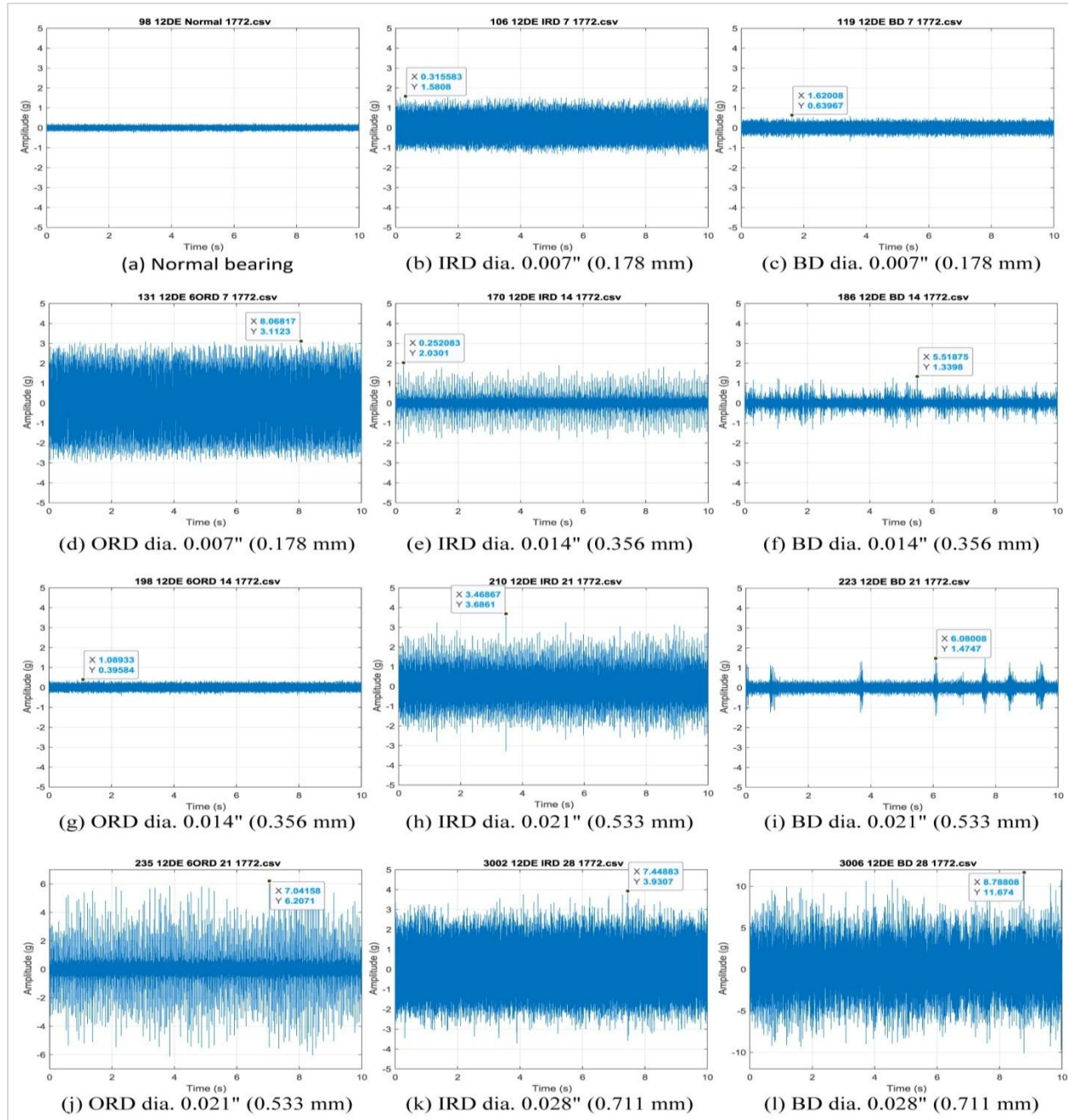
Prashant H. Jain and Santosh P. Bhosle.

Figure 5 Time waveforms of normal and defective bearings at 1772 rpm

Table 9 Values of all indicators for normal and defective bearings at 1772 rpm

Condition Indicators	Normal bearing	IRD sizes				BD sizes				ORD sizes			
		0.007"	0.014"	0.021"	0.028"	0.007"	0.014"	0.021"	0.028"	0.007"	0.014"	0.021"	0.028"
PEAK	0.318	1.581	2.030	3.686	3.931	0.640	1.340	1.475	11.674	3.112	0.396	6.207	NA
RMS	0.066	0.293	0.166	0.442	0.838	0.139	0.141	0.129	2.030	0.592	0.094	0.561	NA
CF	4.785	5.397	12.265	8.343	4.693	4.600	9.510	11.427	5.751	5.258	4.230	11.057	NA
KUR	2.931	5.542	22.084	7.667	3.196	2.964	8.837	9.407	3.910	7.595	2.940	21.971	NA
IF	5.938	7.613	5.752	8.493	5.495	11.038	20.484	13.636	5.285	12.332	15.557	22.191	NA
SF	1.241	1.411	1.250	1.615	1.311	1.462	1.670	1.434	1.249	1.478	1.361	2.007	NA

708

TALAF	0.594	0.998	0.704	1.218	1.226	1.067	1.391	1.040	0.638	1.156	1.055	1.483	NA
THIKAT	2.237	4.014	2.175	4.639	3.950	6.825	16.486	9.000	1.986	7.380	11.124	14.837	NA
KUCR	5.611	24.444	10.081	47.479	53.689	28.623	37.713	22.031	6.648	56.036	24.128	96.031	NA
ECI	0.012	0.475	0.057	2.661	2.913	0.468	0.605	0.175	0.026	1.497	0.157	6.924	NA
SIANA	2.026	4.000	1.991	5.183	2.054	6.976	23.992	8.627	1.879	6.813	9.931	22.484	NA
INTHAR	-0.732	1.769	0.093	4.247	2.444	2.925	7.923	2.120	-0.519	5.028	2.642	18.181	NA
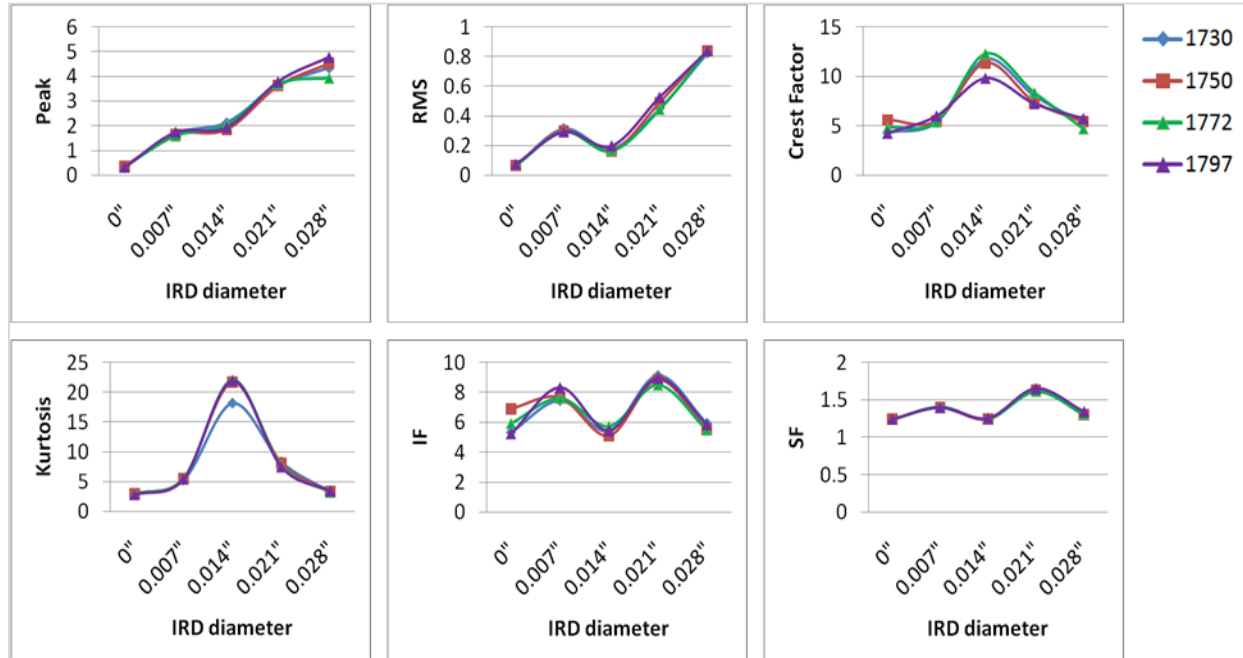
Figure 6 Effect of increase in IRD size on traditional statistical indicators at different speeds

In addition, the characteristic defect frequencies calculated for each defect at different speeds are given in *Appendix II*. Also, the envelope spectrums obtained for normal and defective bearings at 1772 rpm are shown in *Appendix III*. In most of the envelope spectrums of defective bearings, the peaks are seen at shaft rotational frequency (f_s) and at the defect frequencies.

5.Discussion
5.1Effects of change in speed on statistical indicators for normal bearing
Figure 4 shows that for normal bearing, the values of RMS, SF, TALAF and ECI for varying speed between 1730 rpm and 1797 rpm are absolutely flat. However, the values of CF, IF, KUCR, THIKAT, SIANA and INTHAR significantly change with a change in speed. This is because, these indicators depend on the ratio of peak to RMS or the ratio of peak to absolute mean. Therefore, a slight increase in the value of the peak increases the values of these indicators. Impulse factor (IF) is more sensitive to the speed, followed by KUCR and CF. Since the speed range is very small, more comprehensive study of the

709

effect of change in speed on vibration responses is not possible.

Several researchers [1, 11, 14, 40] in their studies observed that the value of kurtosis for normal bearing is close to 3. In this study also, it is observed from *Table 8* and *Figure 4* that for normal bearing the average value of kurtosis is close to 3. Consequently, there is good agreement between the kurtosis values obtained in this study and the kurtosis values observed in the other studies. Additionally, in this study, the average values of CF, TALAF, and THIKAT calculated for normal bearing are near 4.7, 0.6, and 2.18 respectively, which is in good agreement with the values observed by Jain and Bhosle [11]. This also validates the results obtained in this work.

5.2Effects of bearing defect sizes on statistical indicators
Figure 5 shows that for all types of bearing defects and for all defect sizes, the vibration levels and the peak amplitudes are greater than those of the normal bearing. The effects of an increase in bearing defect

sizes of IRD, BD and ORD on dimensional and non-dimensional statistical indicators are analyzed when the motor speed is 1772 rpm.

5.2.1 Effects of increase in bearing defect sizes on dimensional statistical indicators

Peak and RMS are the dimensional statistical indicators whose units are the same as the vibration amplitude. In this paper, the vibration amplitude of each signal is acceleration. *Figure 6* shows that the peak and RMS values reach their maximum levels with the increase in defect size. However, the values of the remaining traditional indicators get reduced to their original levels corresponding to the undamaged ones. For the motor speed of 1772 rpm, *Figure 7* shows changes in peak and RMS values and changes in crest factor (dashed curve) when the diameter of IRD, BD and ORD increases. In the case of a bearing having an IRD or BD (*Figure 7(a)* and *7(b)),* it is seen that when a defect first appears, the peak value increases, whereas the RMS value remains the same. Due to this, the value of the crest factor increases at

the beginning. But, as the size of the defect grows, the RMS value also increases along with the peak value, resulting in a decrease in CF. In the case of a bearing having an ORD *(Figure 7(c)),* it is seen that with the growth of the defect diameter, both peak and RMS values vary. The variation in the peak value is more than that of the RMS value. When the diameter of the defect reaches 0.007 inches, the RMS value also increases with increase in the peak value. Therefore, the CF does not change much. The variation in RMS with peak causes variation in CF. In the case of a bearing having a BD or an ORD, when the bearing element deteriorates more, the peak value increases much faster. From *Figure 7*, it is clear that for all types of defects, peak value gives early intimation about bearing defect occurrence and its deterioration than RMS and CF. Further increases in defect diameter result in a higher RMS value and a larger peak value.
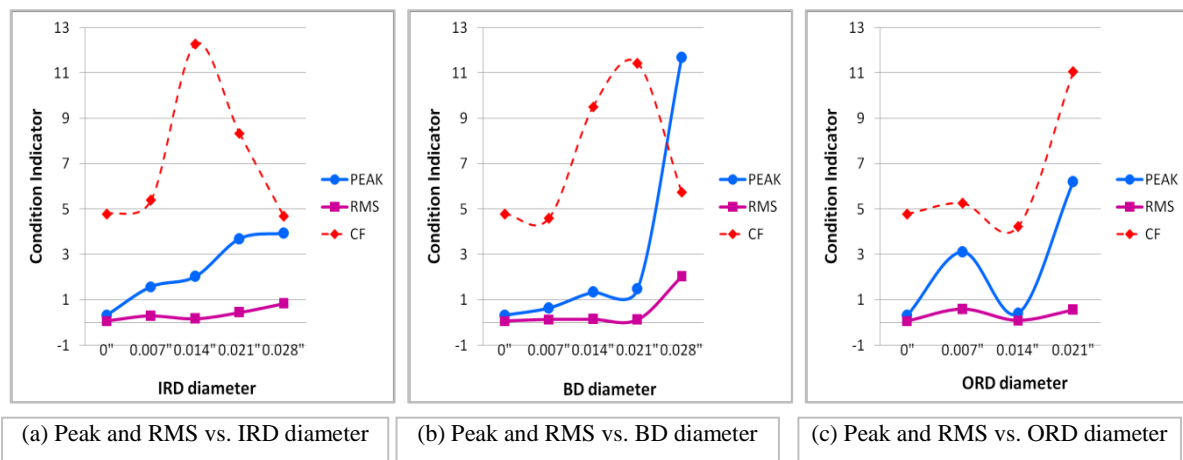

| (a) Peak and RMS vs. IRD diameter | (b) Peak and RMS vs. BD diameter | (c) Peak and RMS vs. ORD diameter |

Figure 7 Peak and RMS values with CF at 1772 rpm for different defect sizes

5.2.2 Effects of increase in bearing defect sizes on non-dimensional statistical indicators

The statistical indicators used in this paper for analysis other than peak and RMS are non-dimensional statistical indicators. These indicators have no unit. *Figures 8, 9* and *10* show the changes in the values of all the non-dimensional indicators for a speed of 1772 rpm for the increasing sizes of IRD, BD and ORD. These figures show the indicator values of the defective bearings presented in *Table 9.* All indicators vary with the change in defect size of the bearing with more or less sensitivity.

From *Figures 8, 9* and *10*, it is clear that for all types of defects, the slope of the KUCR curve is greater than that of other indicator curves when the defect

size increases. Therefore, KUCR is the most sensitive indicator of bearing defects and their size evolution. However, SF and TALAF are less sensitive to defect detection. CF and KUR show a similar relationship with the increase in defect size, but with different levels of sensitivity. Also, IF, SIANA, THIKAT, ITHAR, and ECI have similar relationships for defect size growth with different sensitivity levels.

Figure 8 illustrates that, in the case of bearings that have an IRD, all non-dimensional indicators except KUCR come down to levels that are considered normal. Only KUCR reaches its maximum level when the defect becomes severe. *Figure 9* shows that, in the case of bearings that have a BD, all non-dimensional indicators come down to levels that are

710

considered normal. Only KUCR reaches its maximum level when the defect diameter is 0.014 inches. This level of KUCR is much greater than the maximum levels of other indicators. *Figure 10* shows that, in the case of bearings that have an ORD, all non-dimensional indicators reach to their maximum

levels when the defect becomes severe. KUCR also increases with an increase in the defect size and reaches its maximum level when the defect size becomes severe. But, KUCR increases with greater sensitivity than other indicators.
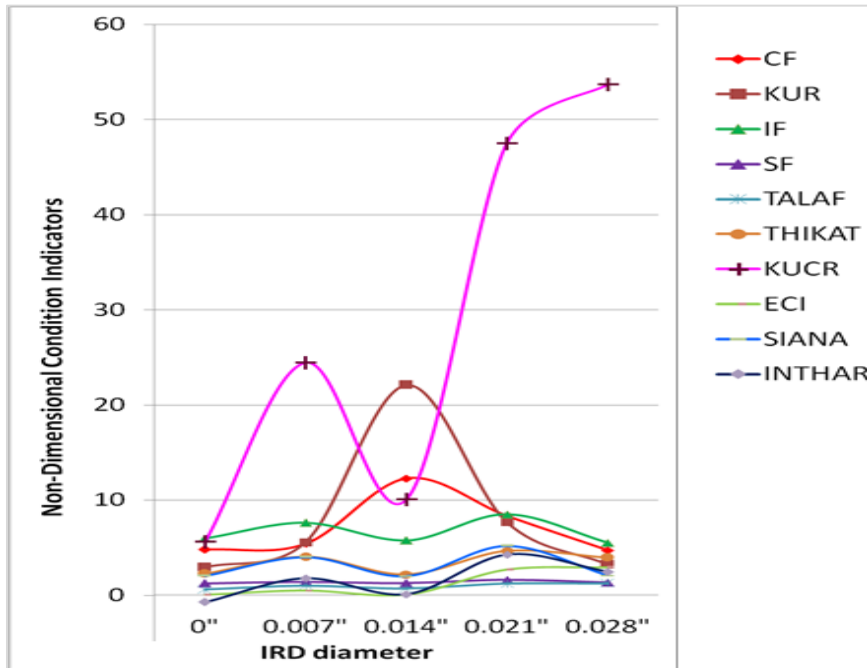
Figure 8 Non-dimensional conditioners vs. IRD diameter
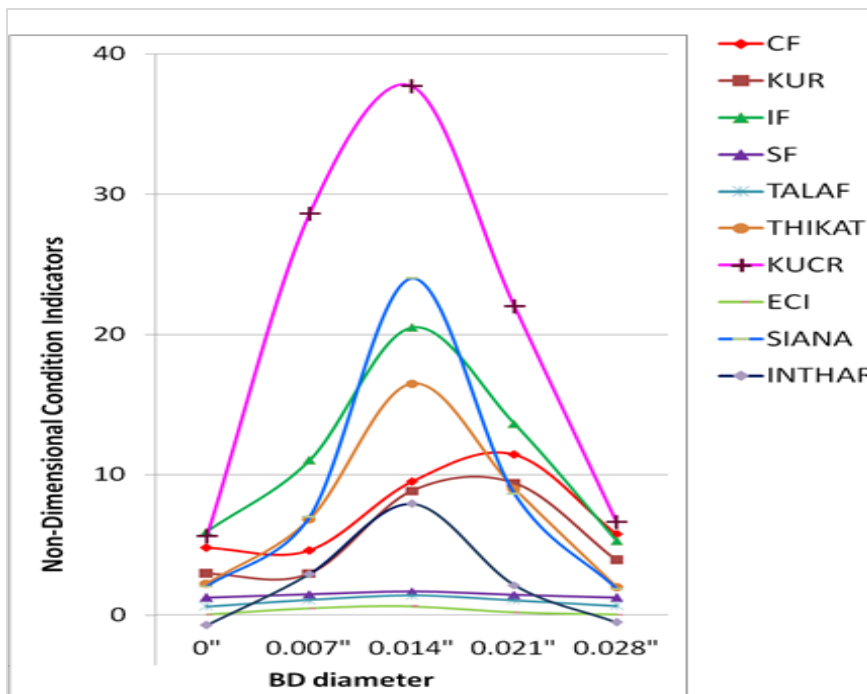
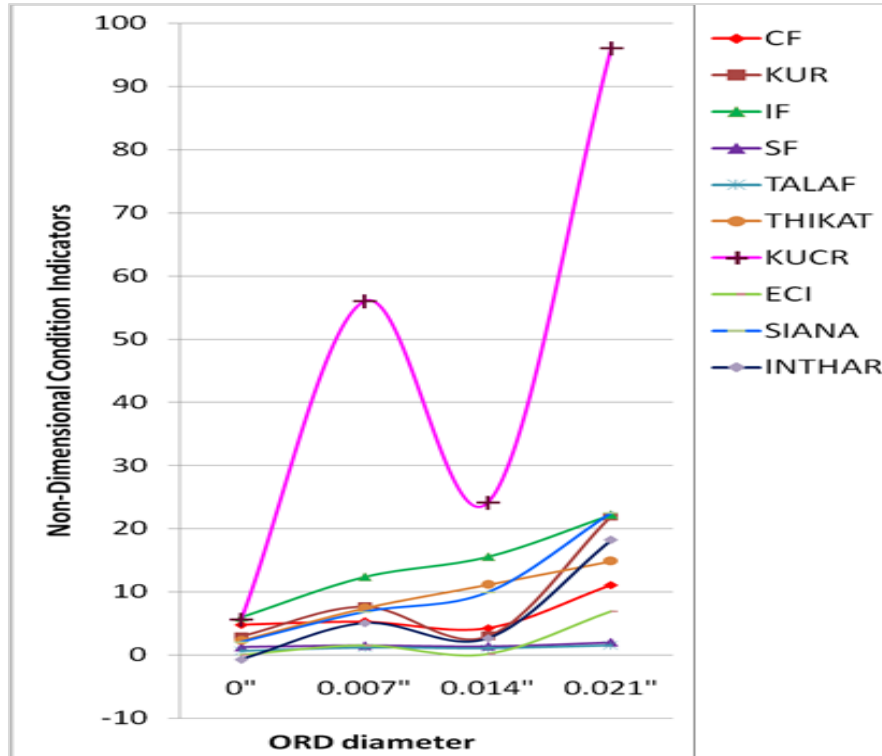**Figure 9** Non-dimensional conditioners vs. BD diameter

711

Figure 10 Non-dimensional conditioners vs. ORD diameter

Though all statistical indicators indicate the presence of defects in the bearings, they are not able to indicate the exact location of the defect present in the bearing. With an increase in bearing defect size, the values of statistical indicators change up and down. Therefore, in the diagnosis of the evolution of defect size, these indicators are useful along with monitoring their trends from the beginning.

5.3 Limitations
In this work, the effects of bearings having an IRD and a BD of 0.028-inch defect diameter on vibration responses are investigated. But, since the dataset of the ball bearing having an ORD of 0.028-inch defect diameter is not available on CWRU's website [37], the analysis of the effect of severe ORD is not possible. Another limitation is that the bearing vibration data is only available for the motor speed between 1730 rpm and 1797 rpm. Since the speed range is very narrow, 66 rpm, it does not allow the study of bearing vibration effects for a wide speed range.

6. Conclusion and future work
In this paper, the effects of various types of bearing defects and their sizes on bearing vibration are analyzed using traditional time-domain statistical indicators and new indicators developed by other researchers. Also, the sensitivity of all indicators is analyzed for the detection of bearing defects and the evolution of the defect size.

Based on this analysis, the following points can be concluded: 1) all the indicators vary with the change in defect size with more or less sensitivity. 2) KUCR is the most sensitive indicator to the detection of incipient defects and the evolution of defect sizes; however, shape factor and TALAF are less sensitive to defect detection. Therefore, it is recommended to use KUCR as a condition indicator monitoring the bearing defects and their sizes. 3) Statistical indicators can indicate the occurrence of bearing defects, but they cannot indicate the exact location of the defects within the bearing, and they are not useful without monitoring vibration trends of bearing from the beginning.

In future, the sensitivity of these statistical indicators can be analyzed for detection of other types of bearing faults such as bearing defect depth, waviness, unbalance, etc.

Engineering Osmanabad (India) and Maharashtra Institute of Technology Aurangabad (India) and for providing the bearing datasets (online), licensed MATLAB software and literature review facilities, respectively.

Conflicts of interest
The authors have no conflicts of interest to declare.

Author's contributions statement
Prashant H. Jain: Conceptualization, planning, literature survey on application bearing vibration analysis techniques, data collection, data processing, presentation of results, analysis of results, discussion of results and writing – original draft. **Santosh P. Bhosle:** Supervision, proof reading, draft manuscript preparation, revision of manuscript.

References
[1] Howard I. A review of rolling element bearing vibration'detection, diagnosis and prognosis'. Canberra, Australia: Defence Science and Technology Organization; 1994.

[2] Sassi S, Badri B, Thomas M. Tracking surface degradation of ball bearings by means of new time domain scalar indicators. International Journal of COMADEM. 2008; 11(3):36-45.

[3] Shukla S, Yadav RN, Sharma J, Khare S. Analysis of statistical features for fault detection in ball bearing. In international conference on computational intelligence and computing research 2015 (pp. 1-7). IEEE.

[4] Nguyen TP, Khlaief A, Medjaher K, Picot A, Maussion P, Tobon D, et al. Analysis and comparison of multiple features for fault detection and prognostic in ball bearings. In fourth European conference of the prognostics and health management society 2018 (pp. 1-9).

[5] Pradhan MK, Gupta P. Fault detection using vibration signal analysis of rolling element bearing in time domain using an innovative time scalar indicator. International Journal of Manufacturing Research. 2017; 12(3):305-17.

[6] Hu A, Xiang L, Zhu L. An engineering condition indicator for condition monitoring of wind turbine bearings. Wind Energy. 2020; 23(2):207-19.

[7] Salem A, Aly A, Sassi S, Renno J. Time-domain based quantification of surface degradation for better monitoring of the health condition of ball bearings. Vibration. 2018; 1(1):172-91.

[8] Paliwal D, Choudhury A, Tingarikar G. Wavelet and scalar indicator based fault assessment approach for rolling element bearings. Procedia Materials Science. 2014; 5:2347-55.

[9] Niu X, Zhu L, Ding H. New statistical moments for the detection of defects in rolling element bearings. The International Journal of Advanced Manufacturing Technology. 2005; 26(11):1268-74.

[10] Tao B, Zhu L, Ding H, Xiong Y. Rényi entropy-based generalized statistical moments for early fatigue defect detection of rolling-element bearing. Proceedings of the Institution of Mechanical Engineers, Part C:

Journal of Mechanical Engineering Science. 2007; 221(1):67-79.

[11] Jain PH, Bhosle SP. Study of effects of radial load on vibration of bearing using time-domain statistical parameters. In IOP conference series: materials science and engineering 2021 (pp. 1-13). IOP Publishing.

[12] Wu Z. Rolling bearing fault evolution based on vibration time-domain parameters. Key Engineering Materials. 2016; 693:1412-8. Trans Tech Publications Ltd.

[13] Jain PH, Bhosle SP. A review on vibration signal analysis techniques used for detection of rolling element bearing defects. SSRG International Journal of Mechanical Engineering. 2021; 8(1):14-29.

[14] Dyer D, Stewart RM. Detection of rolling element bearing damage by statistical vibration analysis. American Society of Mechanical Engineers: Digital Collection.1978; 100(2):229-35.

[15] Tandon N. A comparison of some vibration parameters for the condition monitoring of rolling element bearings. Measurement. 1994; 12(3):285-9.

[16] Patil M, Mathew J, Rajendrakumar P. Application of statistical moments and spectral analysis in condition monitoring of rolling element bearings. International Journal of COMADEM. 2009; 12:31-6.

[17] Utpat A, Ingle RB, Nandgaonkar MR. Response of various vibration parameters to the condition monitoring of ball bearing used in centrifugal pumps. Noise & Vibration Worldwide. 2011; 42(6):34-40.

[18] Chebil J, Hrairi M, Abushikhah N. Signal analysis of vibration measurements for condition monitoring of bearings. Australian Journal of Basic and Applied Sciences. 2011; 5(1):70-8.

[19] Wang YJ, Jiang YC, Kang SQ. The applications of time domain and frequency domain statistical factors on rolling bearing performance degradation assessment. Computer Modeling and New Technologies. 2014; 18(8):192-8.

[20] Sharma A, Amarnath M, Kankar PK. Feature extraction and fault severity classification in ball bearings. Journal of Vibration and Control. 2016; 22(1):176-92.

[21] Singh P, Harsha SP. Statistical and frequency analysis of vibrations signals of roller bearings using empirical mode decomposition. Proceedings of the Institution of Mechanical Engineers, Part K: Journal of Multi-body Dynamics. 2019; 233(4):856-70.

[22] Yadav OP, Pahuja GL. Bearing health assessment using time domain analysis of vibration signal. International Journal of Image, Graphics and Signal Processing. 2020; 10(3):27-40.

[23] Heng RB, Nor MJ. Statistical analysis of sound and vibration signals for monitoring rolling element bearing condition. Applied Acoustics. 1998; 53(1-3):211-26.

[24] De ARG, Da SVSA, Padovese LR. New technique for evaluation of global vibration levels in rolling bearings. Shock and Vibration. 2002; 9(4-5):225-34.

Prashant H. Jain and Santosh P. Bhosle.

[25] Kim EY, Tan AC, Yang BS, Kosse V. Experimental study on condition monitoring of low speed bearings: time domain analysis. Australasian congress on applied mechanics 2007 (pp. 108-13). ACAM.

[26] Sreejith B, Verma AK, Srividya A. Fault diagnosis of rolling element bearing using time-domain features and neural networks. In region 10 and the third international conference on industrial and information systems 2008 (pp. 1-6). IEEE.

[27] Karacay T, Akturk N. Experimental diagnostics of ball bearings using statistical and spectral methods. Tribology International. 2009; 42(6):836-43.

[28] Baiche K, Abderrazak L. A statistical parameters and artificial neural networks application for rolling element bearing fault diagnosis using wavelet transform preprocessing. In 5th international conference on electrical engineering-boumerdes 2017 (pp. 1-6). IEEE.

[29] Nayana BR, Geethanjali P. Analysis of statistical time-domain features effectiveness in identification of bearing faults from vibration signal. IEEE Sensors Journal. 2017; 17(17):5618-25.

[30] Jahagirdar A, Mohanty S, Gupta KK. Study of noise effect on bearing vibration signal based on statistical parameters. Vibroengineering Procedia. 2018; 21:26-31.

[31] Liu J, Xu Z, Zhou L, Yu W, Shao Y. A statistical feature investigation of the spalling propagation assessment for a ball bearing. Mechanism and Machine Theory. 2019; 131:336-50.

[32] Aasi A, Tabatabaei R, Aasi E, Jafari SM. Experimental investigation on time-domain features in the diagnosis of rolling element bearings by acoustic emission. Journal of Vibration and Control. 2021.

[33] Yadav OP, Pahuja GL. An automatic approach to diagnose bearing defects using time-domain analysis of vibration signal. In international conference on advances in electrical and computer technologies 2021 (pp. 1305-19). Springer, Singapore.

[34] Altaf M, Akram T, Khan MA, Iqbal M, Ch MM, Hsu CH. A new statistical features based approach for bearing fault diagnosis using vibration signals. Sensors. 2022; 22(5):1-15.

[35] Buchaiah S, Shakya P. Bearing fault diagnosis and prognosis using data fusion based feature extraction and feature selection. Measurement. 2022.

[36] Bastami AR, Vahid S. A comprehensive evaluation of the effect of defect size in rolling element bearings on the statistical features of the vibration signal. Mechanical Systems and Signal Processing. 2021.

[37] https://engineering.case.edu/bearingdatacenter/download-data-file. Accessed 29 December 2021.

[38] Neupane D, Seok J. Bearing fault detection and diagnosis using case western reserve university dataset with deep learning approaches: a review. IEEE Access. 2020; 8:93155-78.

[39] Smith WA, Randall RB. Rolling element bearing diagnostics using the Case Western Reserve University data: a benchmark study. Mechanical Systems and Signal Processing. 2015; 64:100-31.

[40] Martin HR, Honarvar F. Application of statistical moments to bearing failure detection. Applied Acoustics. 1995; 44(1):67-77.

Prashant H. Jain is a research scholar of Maharashtra Insisitute of Technology Aurangabad. He received M.Tech. (Design Engineering) from Shivaji University, Kolhapur in 2009. He has published more than 10 research papers in peer review journals and authored 3 engineering books. He is presently working as Assistant Professor in Mechanical Engineering at T.P.C.T's college of engineering, Osmanabad (India).
Email: phjain30@rediffmail.com

Dr. Santosh P. Bhosle is Professor in Mechanical Engineering and Director of Maharashtra Institute of Technology Aurangabad. He has obtained his Ph.D. degree in Mechanical Engineering from SRTM University Nanded in 2008. He has published more than 40 research papers in National and International Journals and Conferences. He has received the Gold Medal for being a Topper in all branches of Engineering at M.Tech. (Production Engineering) in Visweswaraiah Technological University Belgaum in the year 2003.
Email: spbhosle2001@gmail.com

Appendix I

S. No.	Abbreviation	Description
1	BD	Ball Defect
2	CF	Crest Factor
3	CRIS	Combined Function of Crest Factor, Root Mean Square, Impact Factor and Standard Deviation
4	CWRU	Case Western Reserve University
5	DAT	Digital Audio Tape
6	ECI	Engineering Condition Indicator
7	IF	Impulse Factor
8	IRD	Inner Race Defect
9	JEM	SKF uses the suffix designation "JEM" for bearings that are used in electric motor applications. The "J" designates a pressed steel cage and "EM" designates electric motor quality as required by most electric motor customers.
10	KUCR	Kurtosis, Crest Factor and Root Mean Square
11	KUR	Kurtosis
12	NA	Not Available
13	NTN	New Technology Network
14	ORD	Outer Race Defect
15	RMS	Root Mean Square
16	SF	Shape Factor
17	SKF	Svenska KullagerFabriken [Swedish Ball Bearing Factory]
18	VSA	Vibration Signal Analysis
19	TALAF, THIKAT, SIANA and INTHAR	These are the names of the new indicators developed by the researchers.

Appendix II
Bearing defect frequencies at different speeds

714

Bearing defect frequencies	Formula	Shaft Speed (N_s) in rpm 1730	1750	1772	1797
Outer Race Defect Frequency (ORDF)	$(nf_s/2)(1-D_b/D_c)$	103.36 Hz	104.56 Hz	105.87 Hz	107.36 Hz
Inner Race Defect Frequency (IRDF)	$(nf_s/2)(1+D_b/D_c)$	156.14 Hz	157.94 Hz	159.93 Hz	162.19 Hz
Ball Defect Frequency (BDF)	$(D_b/D_c)f_s[1-(D_b/D_c)^2]$	135.91 Hz	137.48 Hz	139.21 Hz	141.17 Hz

Appendix III

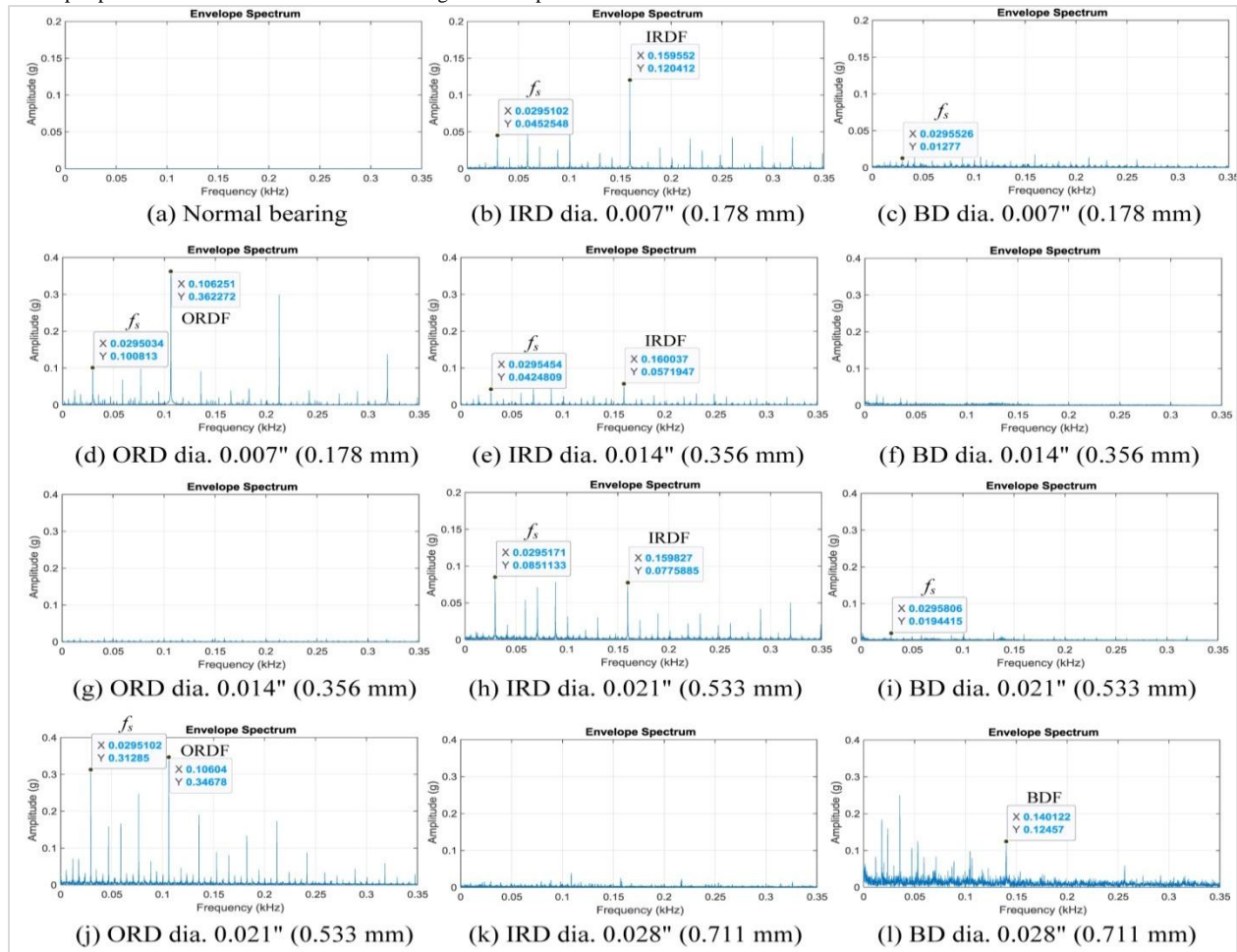Envelope spectrums of normal and defective bearings at 1772 rpm

Figure 11 Envelope spectrums of normal and defective bearings at 1772 rpm